



# Numerical investigation of the dynamic response characteristics of rock mass slopes containing double-hole tunnels subject to seismic excitation

Danqing Song<sup>1,2</sup> · Zhuo Chen<sup>3,4</sup> · Zhizheng Guo<sup>5</sup> · Mengxin Liu<sup>6</sup> · Junfeng Tang<sup>3,4</sup> · Xiangang Jiang<sup>3,4</sup>

Received: 1 May 2022 / Accepted: 16 June 2023 / Published online: 22 June 2023  
© Saudi Society for Geosciences and Springer Nature Switzerland AG 2023

## Abstract

Tunnel–landslide systems are important and difficult engineering problems in tunnel construction. To investigate the dynamic response characteristics of the tunnel-slope system, the seismic response characteristics of layered slopes containing double-hole tunnels at the tunnel portal were investigated using the finite element method (FEM). Two two-dimensional models, including the layered slope (Model 1) and layered slope at the tunnel portal (Model 2), incorporating finite-element meshes with infinite-element boundaries for the models were used in the numerical dynamic analyses. The results show that the lithology of the surrounding rock and the tunnel structure have impacts on the wave propagation characteristics of slopes. Obvious slope elevation and surface dynamic amplification effects can be found. The dynamic amplification effect of the slopes increases with elevation, and the amplification effect of the slope surface is greater than that of the slope interior. In addition, the directions of waves affect the dynamic response of slopes. The vertical wave has a greater impact on the amplification effect of the tunnel structure and bedrock area than the horizontal wave. Horizontal waves have a greater magnification effect in soft and hard rock strata. Moreover, the tunnel structure magnifies the dynamic response of slopes, and the amplification effect of Model 2 to that of Model 1 is 1.0–1.25, overall. The magnification effect of the tunnel structure is mainly concentrated in the adjacent area of the tunnels, and the magnification effect of the left tunnel structure is greater than that of the right structure.

**Keywords** Dynamic response · Tunnel-slope system · Double-hole tunnels · Wave propagation characteristic · Seismic excitation

## Introduction

Landslides at tunnel portals are one of the main geological disasters in tunnel construction and operation (Ergün 2018). The construction of the tunnel project will pass through

steep and complex mountainous areas, and the entrance and exit sections of tunnels face the serious threat of landslide disasters subject to earthquakes (Li et al. 2014; Kaya et al. 2017). The seismic stability of slopes at tunnel portals containing complex geological conditions is particularly prominent. With the rapid development of tunnel engineering, it is also faced with various challenges brought about by the

Responsible Editor: Murat Karakus

✉ Zhuo Chen  
13882535009@163.com

<sup>1</sup> School of Civil Engineering and Transportation, South China University of Technology, Guangzhou 510640, Guangdong, China

<sup>2</sup> State Key Laboratory of Subtropical Building Science, South China University of Technology, Guangzhou 510640, Guangdong, China

<sup>3</sup> College of Civil Engineering, Sichuan Agricultural University, Dujiangyan 611830, Sichuan, China

<sup>4</sup> Sichuan Higher Education Engineering Research Center for Disaster Prevention and Mitigation of Village Construction, Sichuan Agricultural University, Dujiangyan 611830, China

<sup>5</sup> School of Civil and Transportation, Hebei University of Technology, Tianjin 300401, China

<sup>6</sup> Institute of Cold Regions Science and Engineering, School of Civil Engineering, Northeast China Observatory and Research Station of Permafrost Geo-Environment of the Ministry of Education, Northeast Forestry University, Harbin 150040, China

changeable natural environment and complex geological conditions (Zhang et al. 2017; Song et al. 2021a). Tunnel construction inevitably runs through the inner or surrounding areas of the landslide body, causing disturbance to the rock mass and leading to landslide disasters (Fig. 1) (Zhang et al. 2015; Wang et al. 2020a, b). Many traffic tunnels and water diversion tunnels have encountered the deformation problem of the tunnel–landslide system (Bandini et al. 2015). According to the earthquake damage investigation of the 2008 Wenchuan earthquake in China, the tunnel portal section is second only to the severe seismic damage of the tunnel structure at the crossing fault section (Qi et al. 2011; Wang et al. 2014). Therefore, it is of great engineering and scientific significance to investigate the seismic response of the tunnel–landslide system for their seismic fortification of slopes.

The dynamic response characteristics of tunnel-slope systems have been investigated by many scholars. Tunnel-slope systems are very sensitive to seismic waves, which easily cause potential seismic damage. To investigate this phenomenon, Wang et al. (2018) used shaking table model tests to investigate the seismic dynamic characteristics of the tunnel-slope system. Wang et al. (2020a, b) investigated the seismic dynamic response characteristics of the interface between the hard and soft rock of the tunnel-slope system using model tests. Pai and Wu (2021) used the model test method to discuss the spatial deformation characteristics and dynamic response rules of tunnel landslides under potential earthquakes. Su et al. (2022) used a shaking table model test to study the influence of the tunnel structure on the dynamic response characteristics of slopes at the tunnel entrance section. Lei et al. (2023) studied the earthquake failure mechanism and interaction of the tunnel-slope system with a shaking table model experiment. To improve the seismic performance of the tunnel-slope system, Wang et al. (2023) studied the reinforcement measures of the tunnel-slope system and conducted a series of shaking table tests on the tunnel-slope system strengthened by micropiles. Shaking table model tests can simulate the process of earthquake deformation and failure of tunnel-slope systems. Nevertheless, the laboratory model test has the characteristics of a

long test cycle, difficulty in making the model, difficulty in matching the model with the actual slope, and large cost of the test.

The numerical method can be used to analyse the dynamic response of slopes and overcome the above shortcomings. Some scholars have investigated the dynamic response of the tunnel-slope system. Acceleration response has been one of the most direct and effective methods to evaluate the dynamic response of slopes (Chen and Song 2020; Liu et al. 2020). Jiang et al. (2018) investigated the dynamic response characteristics and seismic performance of the tunnel-slope system via the numerical method, and the influence of ground motion directions on the dynamic response of the tunnel-slope system was analysed. Niu et al. (2018) analysed the dynamic response characteristics of a slope with a tunnel by using a numerical method and discussed the influence of ground motion parameters on the dynamic characteristics of the tunnel-slope system. Song et al. (2020) investigated the dynamic response of slopes containing complex geological structures via a numerical method. Fan et al. (2022) studied the influence mechanism of tunnel excavation on slope stability by numerical simulation and revealed the interaction between tunnels and landslides. Zhang et al. (2022) used a numerical method to explore the influence of landslide deformation on the tunnel lining structure and analysed the pile-anchor reinforcement mechanism of the tunnel-slope system. Li et al. (2023) analysed the seismic response of a slope tunnel system by using the boundary integral equation method and explored the dynamic response of tunnels with different section shapes at different frequencies and angles of incidence. Therefore, the numerical method is widely used to study the interaction between tunnels and slope systems.

In addition, the seismic load propagates in the rock mass in the form of seismic waves, which changes its original stress field and easily causes instability and failure of the tunnel-slope system (Konagai et al. 2005; Song et al. 2021a,b). The layered slope is a common geological body in the construction of tunnel engineering, but seismic waves are typical random waves, and the rock–soil mass has the characteristics of nonuniformity, nonlinearity, anisotropy, etc. (Fan et al. 2019). Moreover, due to the complexity of



**Fig. 1** Landslide hazards at tunnel entrance section

the interaction mechanism between discontinuities of rock mass and waves, as well as the interaction between the disturbance of tunnel excavation and the surrounding rock in slopes, the seismic response of the layered slopes at the tunnel portal becomes more complex (Liu et al. 2013). However, research on the dynamic characteristics of tunnel-slope systems containing complex geological structures is insufficient. The dynamic response characteristics of tunnel-slope systems containing double tunnels in composite strata are rarely investigated; in particular, the lack of research on the wave propagation characteristics of the tunnel-slope system is usually ignored. There is a lack of research on the correlation mechanism between composite strata and the seismic response characteristics of tunnel-slope systems containing double-hole tunnels. Hence, it is necessary to further investigate the dynamic response characteristics of the tunnel-slope system containing a double tunnel in composite strata and the interaction mechanism between the tunnel structure and the slopes subject to seismic excitation.

In this work, taking a layered rock slope-tunnel system as an example, two numerical finite-element models were carried out to perform FEM dynamic analyses to investigate the seismic dynamic characteristics of the tunnel-slope system, including the layered slope without a tunnel (Model 1) and the layered rock slope containing double-hole tunnels (Model 2). In addition, by analysing the acceleration response characteristics of the models, the propagation characteristics of seismic waves in the tunnel structure and layered slopes are investigated. According to the analyses of the acceleration response characteristics of the models, the influence of topographic geological factors and the input direction of ground motion on the dynamic amplification effect of the slope and tunnel structure is investigated. By comparing and analysing the two models, the influence mechanism of the tunnel structure on the dynamic response of a layered slope is discussed. The research flow chart of this work is shown in Fig. 2. This work can provide a basis for seismic fortification of tunnel-slope systems.

## Methodology

### Case study

The study area is located in western Sichuan Province, Southwest China, and the geographical location is shown in Fig. 3. There are several fault zones in the study area. The runoff in the area is mainly replenished by alpine snowmelt and rainfall. The pore water and bedrock fissure water constitute the surface water in the area. In the vicinity of the tunnel site, the groundwater is buried relatively deep, and no obvious groundwater outcrops are seen. The study area is located in the suture zone between the Eurasian plate

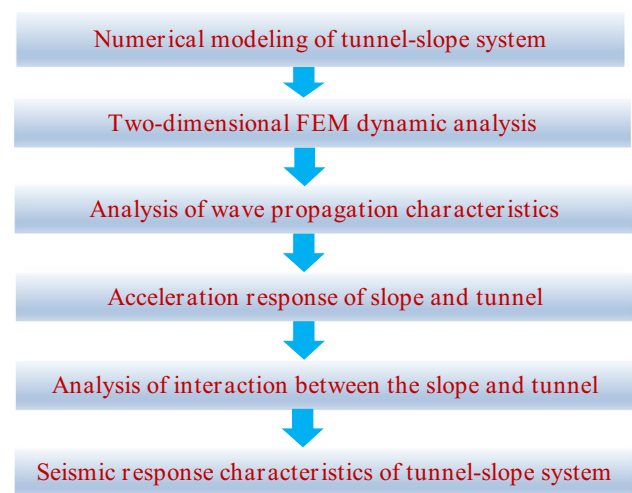


Fig. 2 Research flow chart of this work

and the Indian plate and in the Sichuan-Yunnan block of the Qinghai-Tibet Plateau block, which is mainly affected by the pushing of the Indian plate eastwards and the superposition of the extrusion of the Qinghai-Tibet Plateau southwards. The Sichuan-Yunnan block has a very complex geological structure and belongs to the most intense continental crustal structure in China. The study area is characterized by high intensity and frequency of seismic activity. In recent years, there have been 4 earthquakes of  $M_S$  7.0 and above in the study area. Taking a layered slope at a mountain tunnel portal in the area as an example, the topography and landform are shown in Fig. 4a. The surface relative elevation of the slope at the tunnel entrance section is 15–25 m, and the topographic slope is  $40^\circ$ – $50^\circ$ . The tunnel form is a double-hole tunnel crossing the layered slope. The lithology of the rock mass slope is the bedrock, soft rock, and hard rock from the bottom to the top of the slope. The geological generalization model of the slope is shown in Fig. 4b. Accurate acquisition of the physical and mechanical parameters of rock masses is the basis of seismic stability analysis of tunnel portal sections. The physical and mechanical parameters of the slope and tunnel structure were obtained through a large number of field and laboratory tests, as shown in Table 1.

### Numerical modelling and boundary conditions

To study the seismic response characteristics of the layered slope at the tunnel portal, two finite-element models were established, as shown in Fig. 5. The numerical model is composed of a rock mass and tunnel lining structure, and the rock mass is composed of bedrock, hard rock, and soft rock strata. The sizes of the two models are 34 m (long)  $\times$  22 m (high), and their gradients are approximately  $40^\circ$ . The thicknesses of the hard rock and soft rock are 4 m

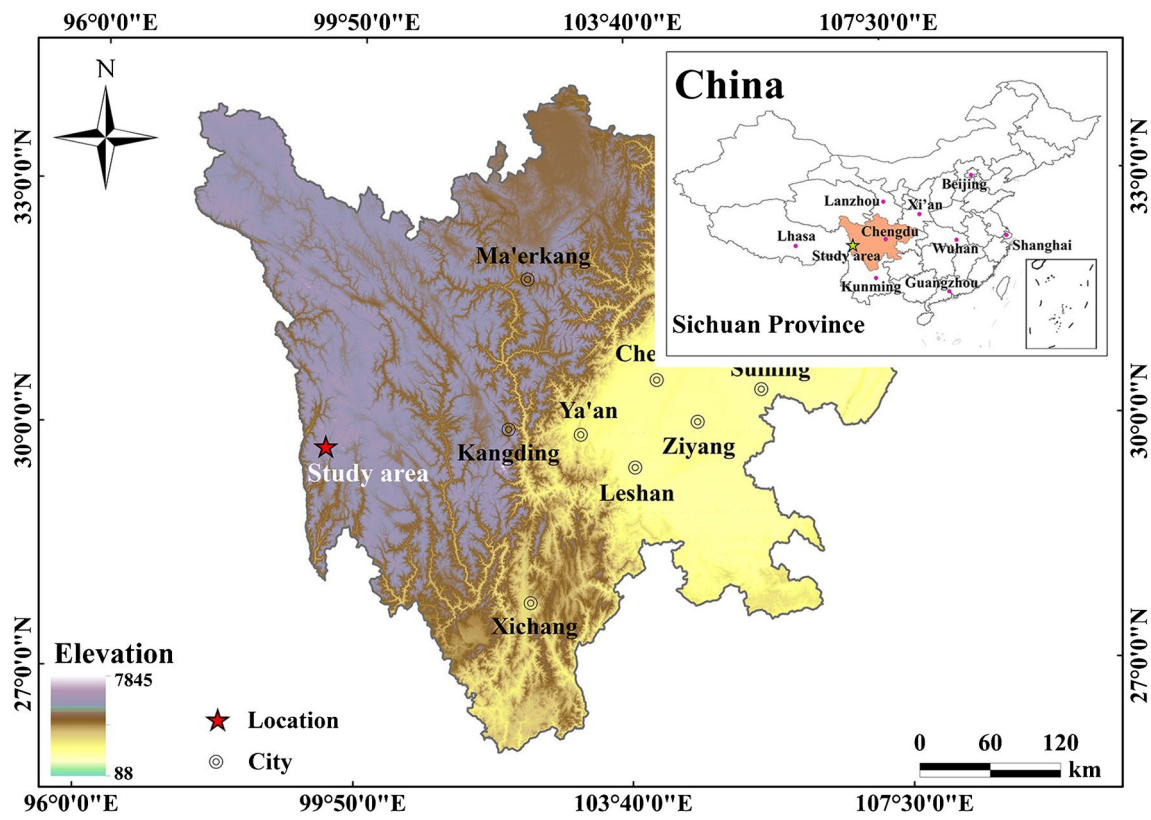


Fig. 3 Location of the study area

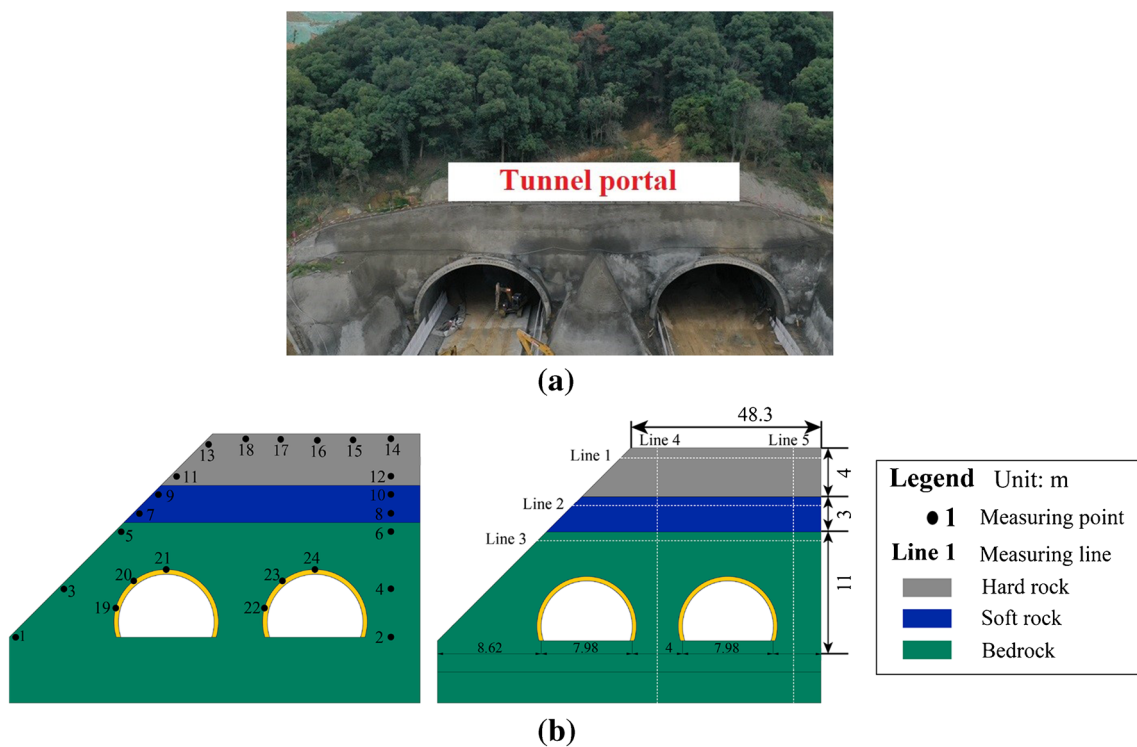


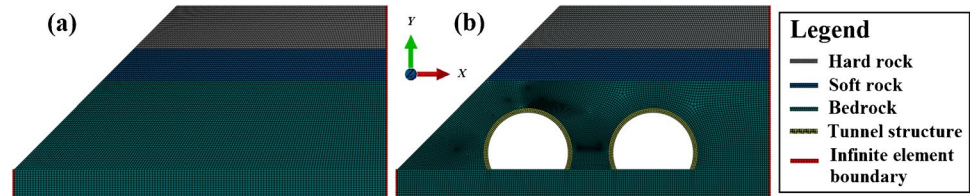
Fig. 4 The layered slope at the entrance section of the tunnel: **a** topography and landform; **b** generalized model of the slope



**Table 1** Physic-mechanical parameters of the model material

Type	Volumetric weight $\rho$ / (kN·m <sup>-3</sup> )	Poisson's ratio $\mu$	Modulus of elasticity $E$ /GPa	Angle of internal friction $\varphi$ (°)	Cohesive forces $c$ /MPa
Bed rock	25.0	0.25	19.23	65.0	1.5
Soft rock	20.0	0.3	1.642	27.0	0.2
Hard rock	23.0	0.3	5.724	50.0	0.7
Lining structure	24.0	0.167	34.5	24.2	0.1

**Fig. 5** Numerical model: **a** Model 1; **b** Model 2



and 3 m, respectively. The propagation of seismic waves in a rock mass can be modelled by assuming that the rock mass medium is continuous or discontinuous. In finite-element dynamic analysis, optimizing the boundary conditions of the numerical model and its degree and subdivision size is of great significance for accurately simulating the mechanism of wave propagation in a discontinuous medium (Song et al. 2020a,b). The stiffness matrix of this joint element is derived by the same method as that of the conventional FEM. The calculation accuracy and efficiency should be considered in the meshing process. Kuhlemeyer and Lysmer (1973) believed that the key research areas should be meshed. When the elastic wave passes through the surface of the structure, part of the energy is transmitted, and part of the energy is refracted, reflected, and converted. Obviously, the amplitudes of transmitted and reflected waves are closely related to the frequency content of the wave, the discontinuous planes, and their length, spacing, thickness, and other geometrical characteristics. In this model, the rock mass part of the slope is set as a quadrilateral grid, the lining structure is set as a double-layer grid, and local grid encryption processing is carried out. A total of 25,469 nodes and 25,876 grids were generated in the finite-element model. In the process of dynamic analysis, the influence of different physical properties of the rock mass on wave propagation characteristics is mainly considered. The “tie connection” method is adopted to set the connection mode between different rock strata as “nonsurface contact” without setting viscous damping.

Boundary conditions are set as the key factors influencing the slope dynamic analysis. The basis of the actual slope is infinite, but in the finite element, the model boundary size is limited; therefore, how to make use of the finite element model to simulate the actual infinite slope foundation makes the results more reasonable for finite-element dynamic

analysis of the important influencing factors. By introducing an artificial boundary, the reflection of waves caused by artificial truncation on the boundary is minimized. In this work, the infinite element boundary method is used to simulate the infinite foundation of the slope. The bottom and both sides of the model are set as the infinite element boundary. The finite element boundary is introduced into the finite element model, the infinite element boundary conditions are adopted on both sides of the model slope and on bedrock, and the infinite element boundary is used to absorb the radiant energy of surface waves and reduce the adverse effects of reflected waves in the dynamic analysis. Seismic waves input seismic load through the nodes at the bottom of the models and use the infinite element to simulate the seismic wave propagation in the far field region and the finite element to simulate the seismic wave propagation in the near field region. In the finite element dynamic calculation, in the case of elastic media, the stress generated by damping follows the following formula (Madsen 1983):  $\sigma_{xx} = -d_p \dot{\mu}_x$ ,  $\sigma_{xy} = -d_s \dot{\mu}_y$ ,  $\sigma_{xz} = -d_s \dot{\mu}_z$ . Here,  $\dot{\mu}_x$ ,  $\dot{\mu}_y$ , and  $\dot{\mu}_z$  represent the vibration velocity. The reflected energy of the P-wave and S-wave can be reduced by setting coefficients  $d_p$  and  $d_s$  in the numerical calculation.

Since only the dynamic response characteristics of the slope under the condition of small deformation are studied, the materials of the model are regarded as elastic materials in the finite-element dynamic analysis. The dynamic response characteristics of the slope in the linear elastic domain are considered emphatically. The rock mass and structural materials adopt the Mohr–Coulomb criterion. To study the dynamic response characteristics of layered slopes at the tunnel portal section, the Wenchuan seismic wave recorded by the China Wudu Seismic Station in 2008 was loaded in the numerical models. The acceleration-time

history and Fourier spectrum of the WE wave are shown in Fig. 6. Horizontal and vertical WE waves (0.1 g) were used to load the bottom boundary of the models. The predominant frequency of the WE wave is 7.74 Hz, and the input duration time is  $T = 120$  s.

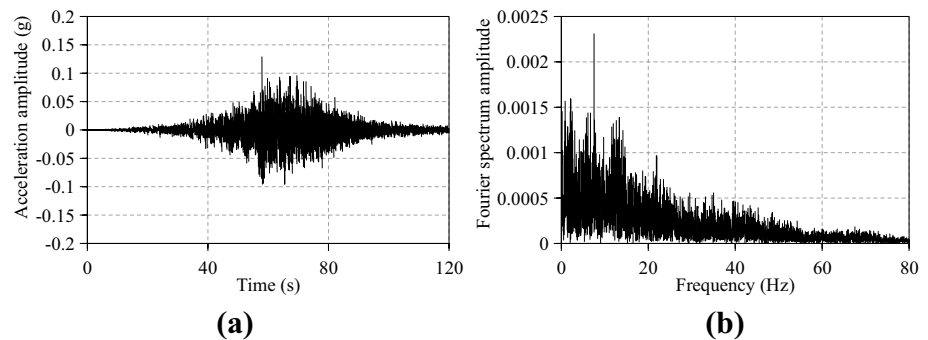
## Results

### Seismic wave propagation characteristics in the layered slope at the tunnel portal

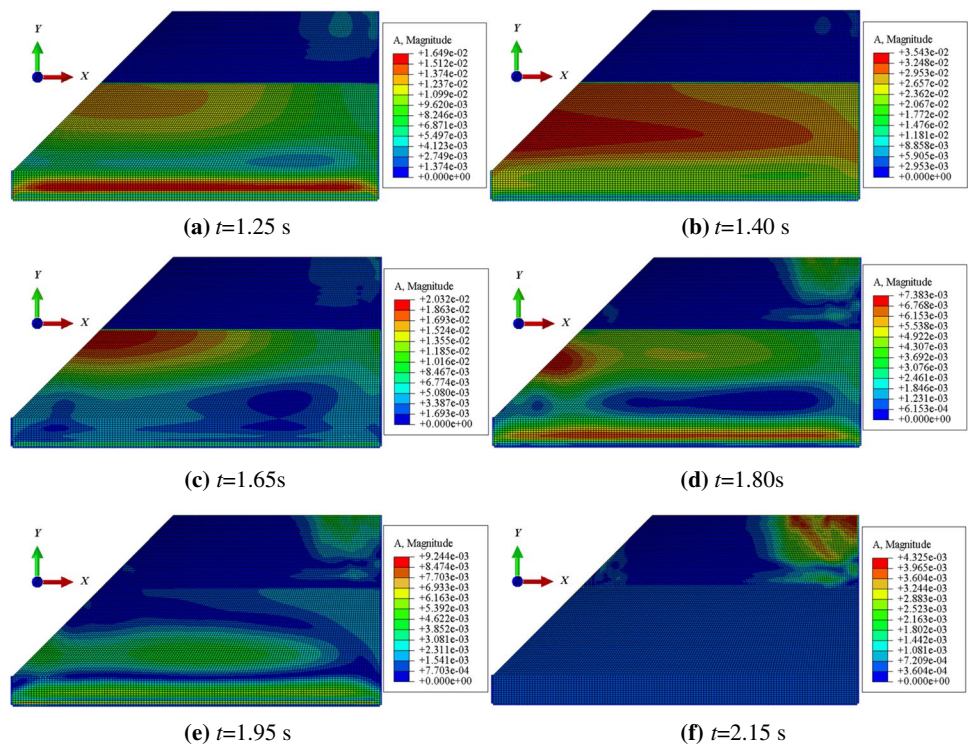
Taking Models 1 and 2 as examples, a certain wave propagation process from the bottom to the slope crest was selected to investigate the propagation characteristics of waves in the slopes. Their acceleration distribution characteristics are shown in Figs. 7 and 8. Layered

propagation characteristics of waves along the elevation in the bedrock area can be found (Fig. 7). When waves propagate to the interface between soft rock and bedrock, due to the reflection and refraction of waves on the discontinuity surface, an obvious phase difference of waves occurs near the discontinuity surface, resulting in the local amplification effect of waves. When the wave propagates to the soft rock and the hard rock, waves no longer show layered propagation characteristics but gradually propagate to the infinite element boundary at the slope crest, which indicates that the difference in rock properties in the slope changes the wave propagation path. In the bedrock area below the tunnel, waves show layered propagation characteristics (Fig. 8). When waves propagate to the tunnel area, waves produce obvious refraction and reflection effects, leading to a local amplification phenomenon between the two tunnels. When waves propagate

**Fig. 6** Wenchuan earthquake waves (0.1 g): **a** acceleration-time history cure; **b** Fourier spectrum



**Fig. 7** Wave propagation characteristics of the Model 1 when input 0.1 g WE wave in-x direction



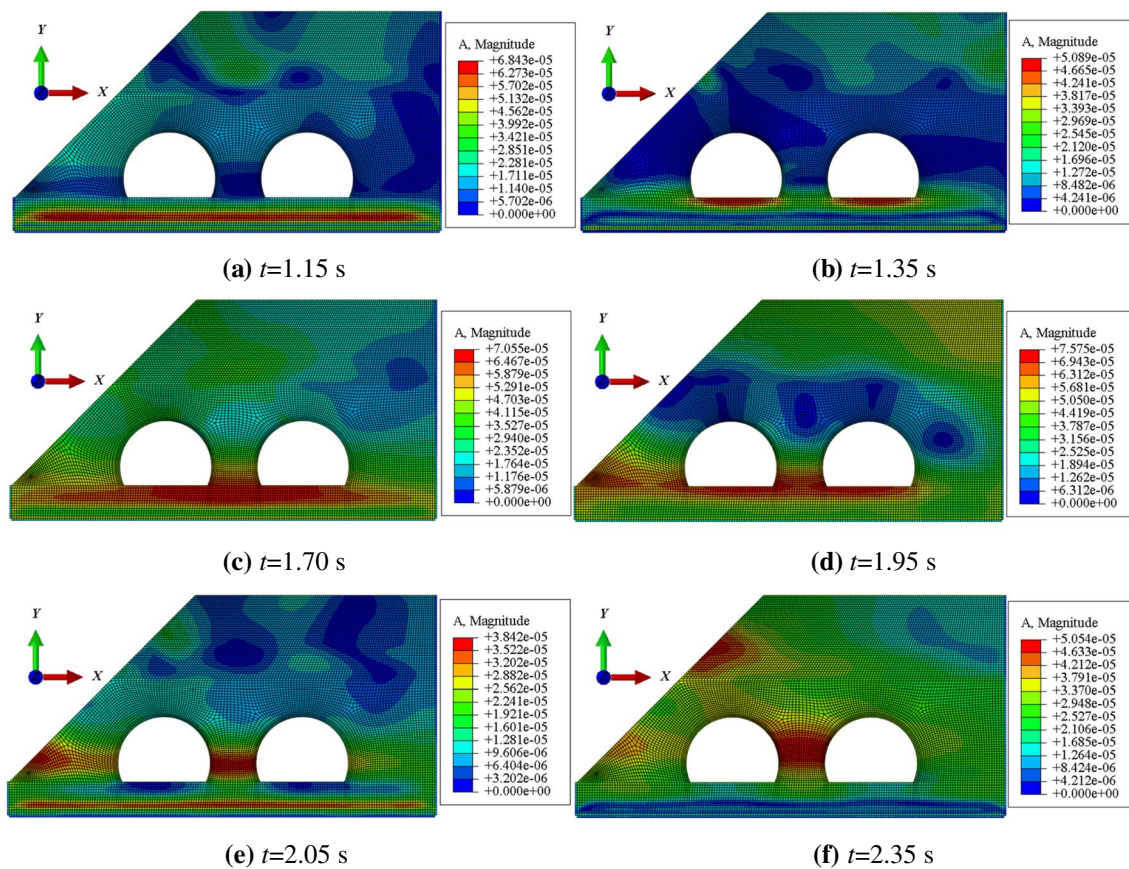


**Fig. 8** Wave propagation characteristics of the Model 2 when input 0.1 g WE wave in-x direction

to soft rock and hard rock, waves show the amplification phenomenon along the slope surface. By comparing Figs. 7 and 8, due to the influence of tunnel excavation, the tunnel structure changes the wave propagation path and characteristics of the slope.

In addition, to further clarify the wave propagation characteristics in the tunnel structure under ground motion, the acceleration distribution characteristics of the lining structure in Model 2 are shown in Fig. 9. Waves start to propagate at the arch foot. With increasing ground motion time, the wave propagates along the lining structure to the waist and the top of the arch. However, the wave propagation characteristics of the left and right lining structures show a difference in the models. This is because the discontinuity between the lining structure and the surrounding rock mass leads to the discontinuity of wave propagation characteristics. In other words, the propagation process of waves in the lining structure shows the discontinuity of propagation characteristics. Hence, the geological conditions and tunnel structure influence the wave propagation characteristics through the slope and change the wave propagation law and the dynamic response characteristics of the slope.

### Dynamic response characteristics of the tunnel-slope system

#### Analysis parameter selection

To investigate the seismic response characteristics of the tunnel-slope system, several typical measuring points on the slope surface and inside the slope were selected for the research object, and their acceleration-time histories under a 0.1 g horizontal wave are shown in Fig. 10. The corresponding acceleration-time histories of the tunnel lining structures are shown in Fig. 11. Figures 10 and 11 show that the slope and tunnel structure have different acceleration-time histories at different locations; that is, the seismic acceleration response characteristics at different locations are significantly different. To study the dynamic response characteristics of the slopes and tunnel structure, the peak ground acceleration (PGA) of different monitoring locations was selected for analysis parameters. However, to further clarify the physical meaning of the acceleration amplification effect, the acceleration amplification coefficient  $M_{PGA}$  is used for the analysis parameters, where  $M_{PGA} = PGA_i / PGA_0$ , and  $PGA_i$  represents the



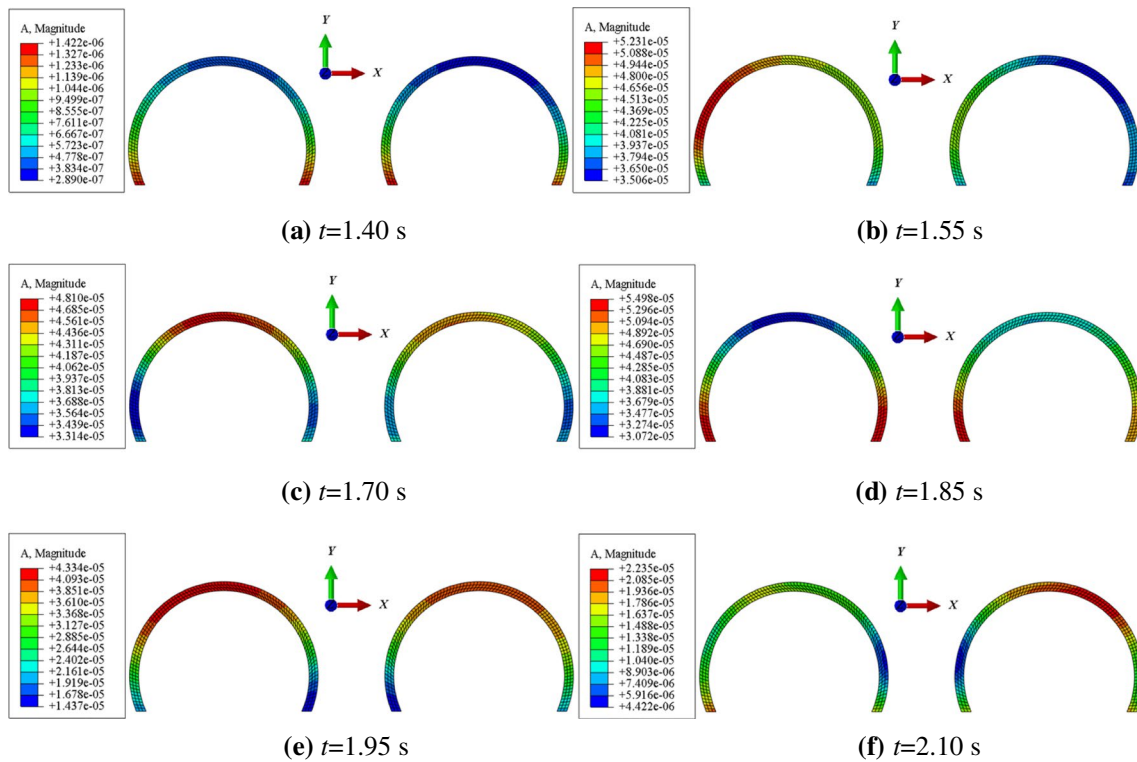


**Fig. 9** Wave propagation characteristics of the tunnel structure of the Model 2 when input 0.1 g WE wave in-x direction

**Fig. 10** Acceleration-time history of the typical measurement points in the Model 2 when input 0.1 g WE wave in-x direction: **a** inside the slope; **b** at the slope surface

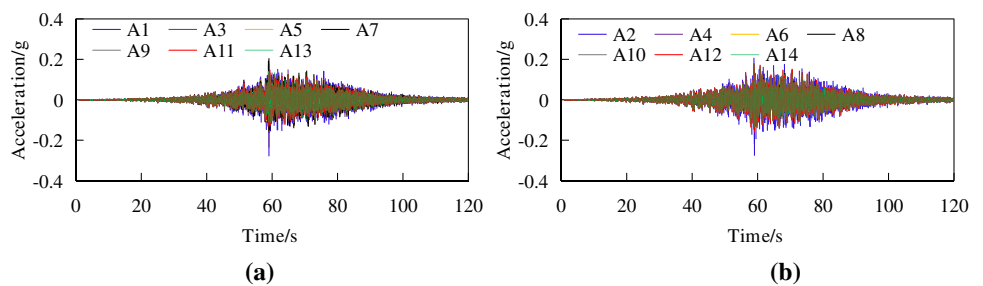
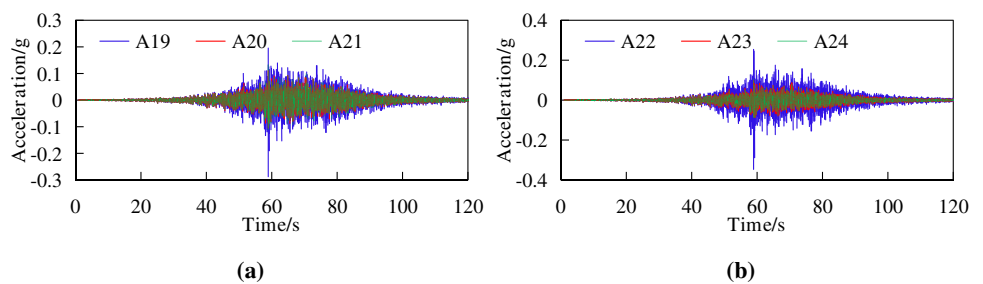


**Fig. 11** Acceleration-time history of the typical measurement points of the tunnel structure in Model 2 when input 0.1 g WE wave in-x direction



peak ground motion acceleration at a certain point (*i*) in the slope.  $PGA_0$  represents the peak ground motion acceleration of the slope toe.  $M_{PGA}$  represents the acceleration magnification effect at a point in the slope. The  $M_{PGA}$  is used to investigate the dynamic response of layered slopes and tunnel structures.

### Influence of topography and geological conditions on the dynamic response of the slopes

During the earthquakes, the buildings at the top of the slope in the mountain area suffered more damage than those at the bottom of the slope, which indicates that surface topography



plays an important role in surface movement (Geli et al. 1988). The complex geological conditions make the propagation characteristics of waves in the rock mass of the slope appear to have great differences, resulting in the different seismic dynamic response characteristics of slopes. Topography and geological factors play an important role in the seismic response of slopes. To clarify their effects on the seismic response of the slopes, taking the input 0.1 g WE

wave as an example, the change rule of the  $M_{PGA}$  in the models under horizontal and vertical waves with elevation is shown in Figs. 12, 13, 14, and 15. Lines 1–3 represent horizontal measuring lines in the hard rock, soft rock, and bedrock, respectively (Fig. 4b). Lines 4 and 5 are the vertical measuring lines of the slopes. Line 4 is located between the two tunnels, and Line 5 is located on the right-most side of the slopes. The relative elevation  $h/H$  refers to the ratio

**Fig. 12**  $M_{PGA}$  variation rule of Model 1 with the elevation when input 0.1 g WE wave in-x direction: (a) along the horizontal direction of the slope; (b) along the vertical direction of the slope

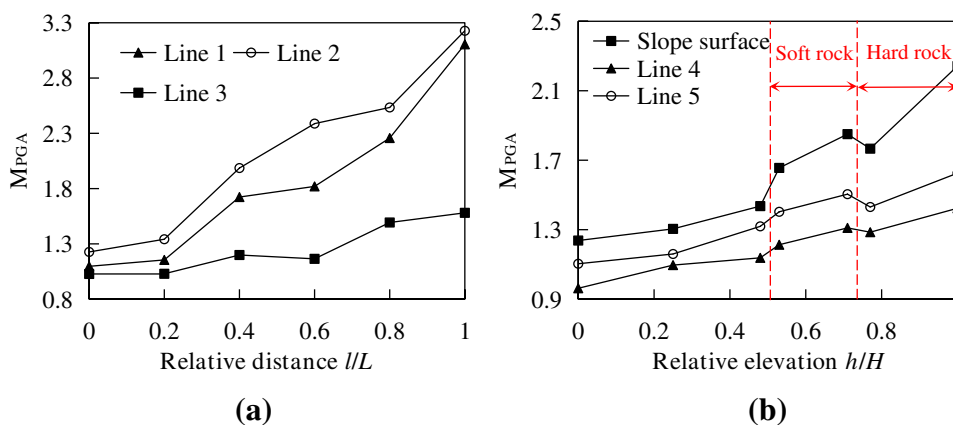


**Fig. 13**  $M_{PGA}$  variation rule of Model 1 with the elevation when input 0.1 g WE wave in-z direction: (a) along the horizontal direction of the slope; (b) along the vertical direction of the slope

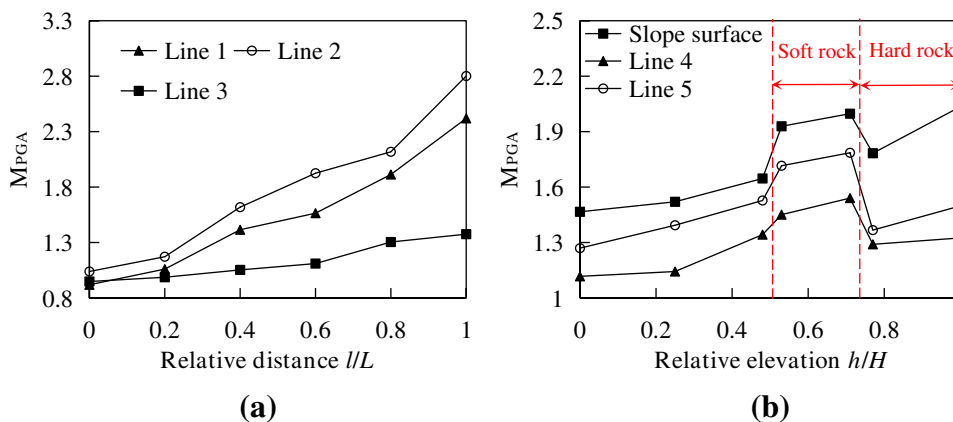


**Fig. 14**  $M_{PGA}$  variation rule of Model 2 with the elevation when input 0.1 g WE wave in-x direction: (a) along the horizontal direction of the slope; (b) along the vertical direction of the slope

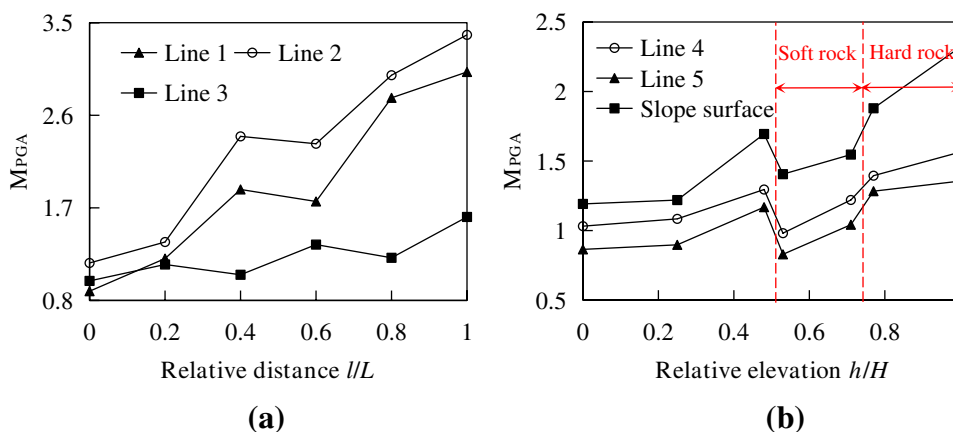
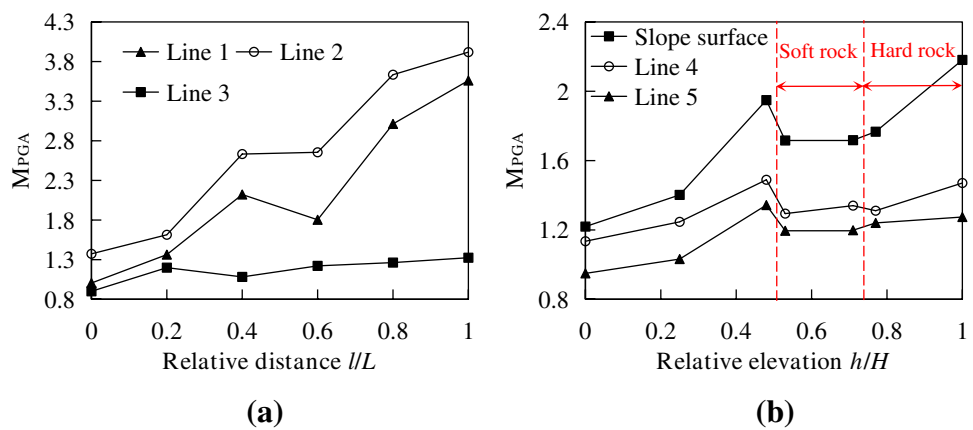


**Fig. 15**  $M_{PGA}$  variation rule of Model 2 with the elevation when input 0.1 g WE wave in-z direction: (a) along the horizontal direction of the slope; (a) along the vertical direction of the slope



of elevation  $h$  of a certain point to the total elevation  $H$  of the slope. The relative horizontal distance  $l/L$  is the ratio of the length  $l$  from the right boundary of a certain point to the slope length  $L$  at a certain elevation. In Figs. 12, 13a, the  $M_{PGA}$  of the three measuring lines in Model 1 gradually increases along the horizontal distance under horizontal and vertical seismic waves; that is, the closer the distance is to the slope surface, the greater the dynamic amplification effect, and the maximum is reached on the slope surface. In Figs. 14, 15a, the  $M_{PGA}$  of the three horizontal measuring lines in Model 2 under horizontal and vertical seismic forces shows a nonlinear increasing trend along the horizontal distance of the model. This is because the existence of the tunnel structure makes the seismic wave propagation characteristics in the slope significantly change, leading to changes in the dynamic amplification effect of the slope.

In addition, Figs. 12, 13b show that the  $M_{PGA}$  of the vertical measuring lines of Models 1 and 2 under horizontal and vertical seismic forces increases as the elevation increases overall and reaches a maximum at the slope crest, indicating that the models have an obvious elevation dynamic amplification effect. The  $M_{PGA}$  increases rapidly when bedrock passes into soft rock strata in Model 1 but decreases to some extent when the soft rock strata transition to hard rock

strata. Figures 14, 15b show that in Model 2, the  $M_{PGA}$  on both sides of the interface between bedrock and soft rock decreases, while the  $M_{PGA}$  on the interface between hard and soft rock strata increases rapidly to a certain extent, indicating that the lithologic difference within the slope body has a great influence on the seismic amplification effect of the slopes. Moreover, in Figs. 12, 13, 14, and 15, the  $M_{PGA}$  of the slope surface in the two models is the largest, indicating that the dynamic amplification effect of the slope surface is the most obvious. To further investigate the slope surface effect of the models, the  $M_{PGA}$  ratio of the slope surface to the internal slope of Models 1 and 2 is shown in Figs. 16, 17. Figures 16, 17 show that under the horizontal and vertical seismic forces, the  $M_{PGA}$  ratio of the models is greater than 1.0 overall as the elevation increases and reaches a maximum at the top slope. This suggests that the two models have a clear slope surface dynamic amplification effect, and the slope surface effect has an obvious elevation amplification effect. The above analysis is consistent with the results of the shaking table model tests of the tunnel-slope system. The topographic and geological conditions have an obvious influence on the dynamic amplification effect under earthquakes (Jiang et al. 2018). Therefore, the models have obvious elevation and slope surface amplification effects,

**Fig. 16**  $M_{PGA}$  ratio of slope surface to internal slope in Model 1 when input 0.1 g WE wave: a input in-x direction; b input in-z direction

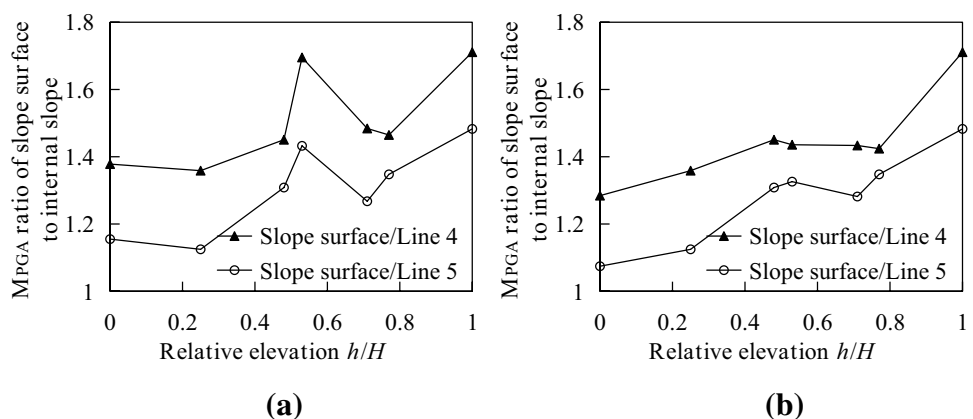
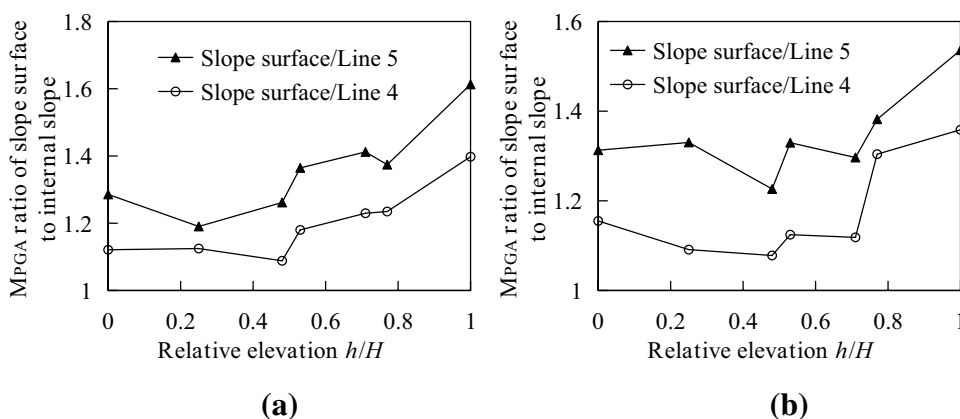


**Fig. 17**  $M_{PGA}$  ratio of slope surface to internal slope in Model 2 when input 0.1 g WE wave: **a** input in-x direction; **b** input in-z direction



the grade of the surrounding rock has an influence on the dynamic amplification effect of the slope, and the soft rock has the most obvious amplification effect.

**Influence of ground motion direction on dynamic response of the slopes**

Different incident directions of waves lead to different propagation paths and characteristics of waves in rock slopes, which results in obvious differences in the seismic response characteristics of the slopes. To study the influence of the input direction of ground motion on the dynamic response of the layered slope at the tunnel portal section, the input horizontal and vertical 0.1 g WE waves were taken as an example. The  $M_{PGA}$  ratios ( $M_{PGA_x}/M_{PGA_z}$ ) of the two models are shown in Figs. 18 and 19. where  $M_{PGA_x}$  and  $M_{PGA_z}$  represent acceleration amplification coefficients under horizontal and vertical seismic forces, respectively. Figures 18 and 19 show that in Model 1, the  $M_{PGA_x}/M_{PGA_z}$  is greater than 1.0 overall, in particular, it is between 1.03 and 1.15 along the horizontal direction of the slope body and between 0.98 and 1.26 along the vertical direction of the slope.  $M_{PGA_x}/M_{PGA_z}$  has a gradually increasing trend with elevation and reaches a maximum at the top slope. This indicates that the  $M_{PGA}$  of

the layered slope under horizontal seismic force is greater than that of the vertical seismic force, and the dynamic amplification effect of horizontal seismic force along the elevation is more obvious.

In addition, in Model 2, the variation trend of the  $M_{PGA_x}/M_{PGA_z}$  along the horizontal direction of the slope is different from that of Model 1. The  $M_{PGA_x}/M_{PGA_z}$  of measuring Line 3 is 1.1–1.2, while the  $M_{PGA_x}/M_{PGA_z}$  ratio of Lines 1 and 2 is less than 1.0 overall. This indicates that the dynamic acceleration amplification effect of the horizontal seismic force is smaller than that of the vertical seismic force in bedrock, while the amplification effect of the horizontal seismic force is greater than that of the vertical seismic force in soft and hard rock strata. In the vertical direction of Model 2, the  $M_{PGA_x}/M_{PGA_z}$  of Lines 4 and 5 gradually decreases with increasing elevation in bedrock, but the  $M_{PGA_x}/M_{PGA_z}$  is greater than 1.0. However, in soft and hard rock strata, the  $M_{PGA_x}/M_{PGA_z}$  increases gradually and is less than 1.0 overall. Moreover, the  $M_{PGA_x}/M_{PGA_z}$  of the tunnel structure in Model 2 is less than 1.0 as a whole, which indicates that the vertical seismic force is more responsive to the dynamic response of the tunnel structure than that of the horizontal seismic force. Comparing Model 2 to Model 1, the existence of the tunnel structure makes the effect of the ground motion

**Fig. 18** Ration of  $M_{PGA_x}$  to  $M_{PGA_z}$  in Model 1 when input 0.1 g WE wave: **(a)** along the horizontal direction of the slope; **(b)** along the vertical direction of the slope

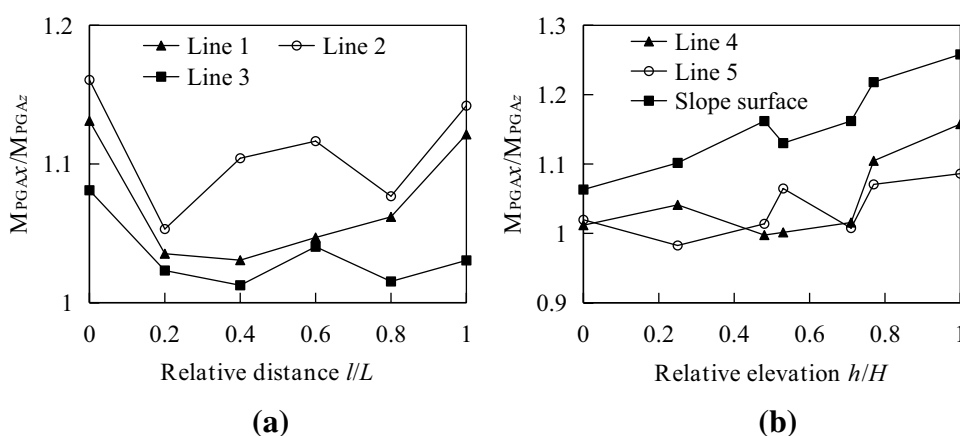
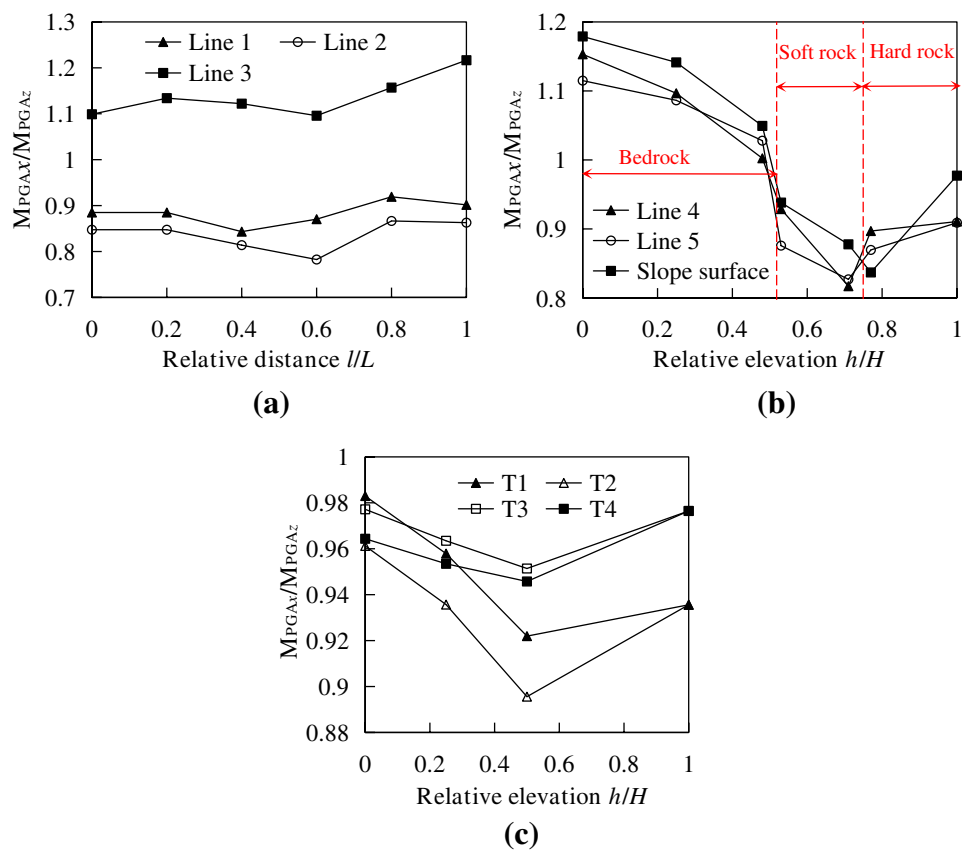


**Fig. 19** Ration of  $M_{PGA_x}$  to  $M_{PGA_z}$  in Model 2 when input 0.1 g WE wave: (a) along the horizontal direction of the slope; (b) along the vertical direction of the slope; (c) tunnel structure



input direction on the dynamic amplification effect of the layered slope appear to change; in particular, it has the largest influence on the amplification effect of the bedrock area containing the tunnel structure. Compared with the dynamic response of the slope, the tunnel structure has a larger impact on the dynamic response of the slope under vertical seismic force than that under horizontal seismic force. This is similar to the results of laboratory model tests (Jiang et al. 2018; Niu et al. 2018; Wang et al. 2018). The numerical simulation and model test reveal the influence of the ground motion direction on the dynamic response characteristics of the slope tunnel system.

#### Dynamic response characteristics of the tunnel structure

For the tunnel-slope system containing two tunnels, the seismic response characteristics of the tunnel structures are more complex. To investigate their seismic response characteristics, the changes in the  $M_{PGA}$  in the two tunnel structures with increasing elevation in Model 2 under horizontal and vertical 0.1 g WE seismic waves are shown in Fig. 20. T1 and T2 represent the lining structures on the left and right sides of the left tunnel, respectively, while T3 and T4 represent the lining structures on the left and right sides of the right tunnel, respectively. The  $M_{PGA}$  of T1 and T4 increases with increasing elevation and reaches the maximum value

at the tunnel vault. The  $M_{PGA}$  of T2 and T3 first increased and then decreased with increasing elevation, and the maximum  $M_{PGA}$  ( $M_{PGAmax}$ ) appeared at the waist of the arch. The  $M_{PGA}$  of T2 and T3 is obviously larger than that of T1 and T4. Meanwhile, the  $M_{PGA}$  of T2 is larger than that of T3. For example, the  $M_{PGAmax}$  values of T2 and T3 under vertical seismic force are approximately 1.61 and 2.12, while the  $M_{PGAmax}$  values of T1 and T3 are approximately 1.35 and 1.33, respectively. In other words, the  $M_{PGA}$  of the right arch waist of the left tunnel structure and the left tunnel arch waist of the right tunnel structure is larger, and the  $M_{PGA}$  of the right arch waist of the left tunnel is the largest.

To further analyze the seismic response characteristics of the two tunnel lining structures, the displacement and Mises stress distribution of the tunnel structure in Model 2 with an input 0.1 g horizontal WE wave are shown in Fig. 21. The displacement and Mises stress of the slope at the tunnel portal are mainly concentrated in the local area between the two tunnels, and the maximum displacement and Mises stress of the tunnel structure are mainly concentrated in the arch waist of the left and right tunnels, which is consistent with the results of acceleration response analysis. Therefore, the dynamic amplification effect of the tunnel lining structure is mainly concentrated in the adjacent area between the left and right tunnels, and the dynamic amplification effect of the left tunnel is greater than that of the right tunnel. In particular,



**Fig. 20**  $M_{PGA}$  of the two-tunnel structure in Model 2 with the elevation when input 0.1 g WE wave: **a** input in-x direction; **b** input in-z direction

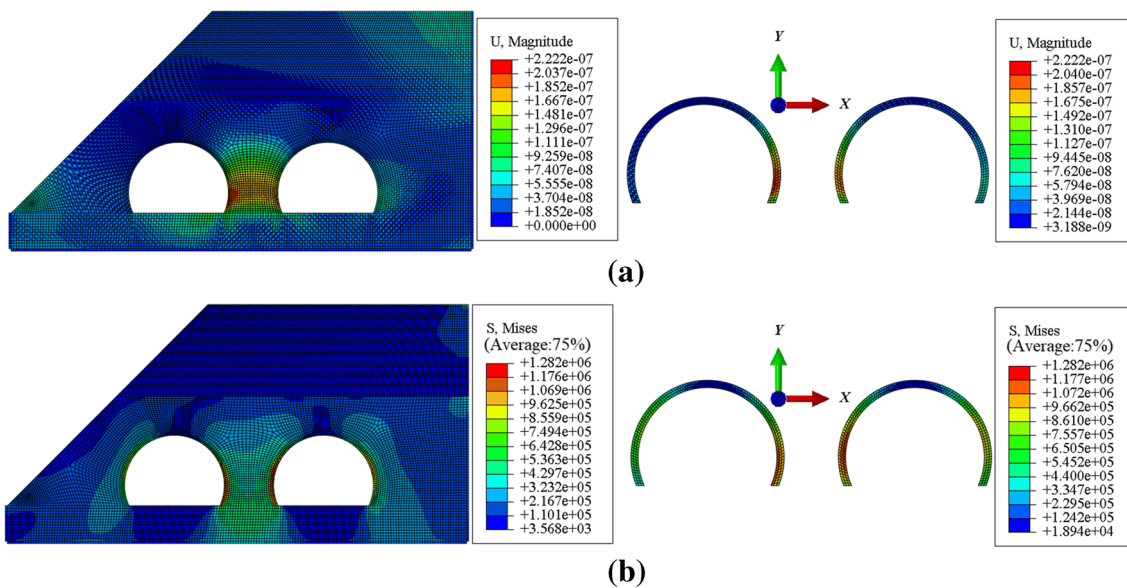
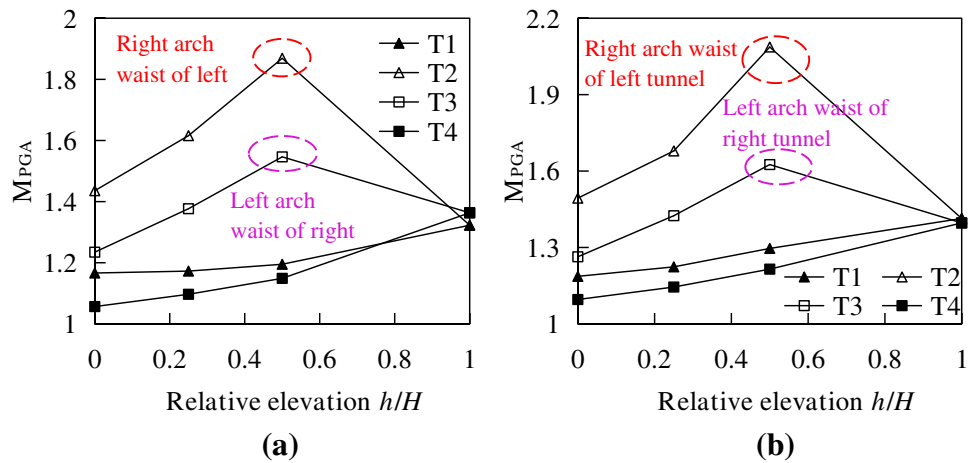


**Fig. 21** Displacement and equivalent stress distribution of the two tunnel structure and Model 2 when input 0.1 g WE wave in-x direction: **a** Displacement; **b** equivalent stress

the seismic dynamic amplification effect of the right arch waist of the lining structure near the slope is the largest.

**Discussion: influence of the tunnel structure on the dynamic response of the slopes**

Due to the difference in lithology and the randomness of seismic waves, the seismic dynamic response characteristics of layered slopes are complex. In particular, the interaction mechanism between the tunnel structure and layered slope is more complex after tunnel excavation, which is difficult to fully understand. The tunnel structure changes the propagation characteristics and path of seismic waves in the rock mass, especially the wave propagation characteristics in

the bedrock area, leading to an obvious local amplification effect between the tunnel structures. In addition, the  $M_{PGA}$  of Model 2 is greater than that of Model 1 under the same conditions, which suggests that the tunnel structure has a significant amplification effect on the dynamic response of the layered slope. By comparing the changes in the  $M_{PGA}$  on the vertical measuring lines and slope surface of Models 1 and 2, there is a certain difference in the increasing trend of the  $M_{PGA}$  in the vertical direction between Model 2 and Model 1. At the same time, the order of the  $M_{PGA}$  of Model 1 is as follows: surface slope > Line 5 > Line 4; however, in Model 2, the corresponding  $M_{PGA}$  order is as follows: slope surface > Line 4 > Line 5. This suggests that the tunnel structure has a significant influence on the dynamic response characteristics of the layered slope. The reason is that the

**Fig. 22**  $M_{PGA}$  ratio of Model 2 to Model 1 when input 0.1 g WE wave in- $x$  direction: **a** along the horizontal direction of the slope; **b** along the vertical direction of the slope

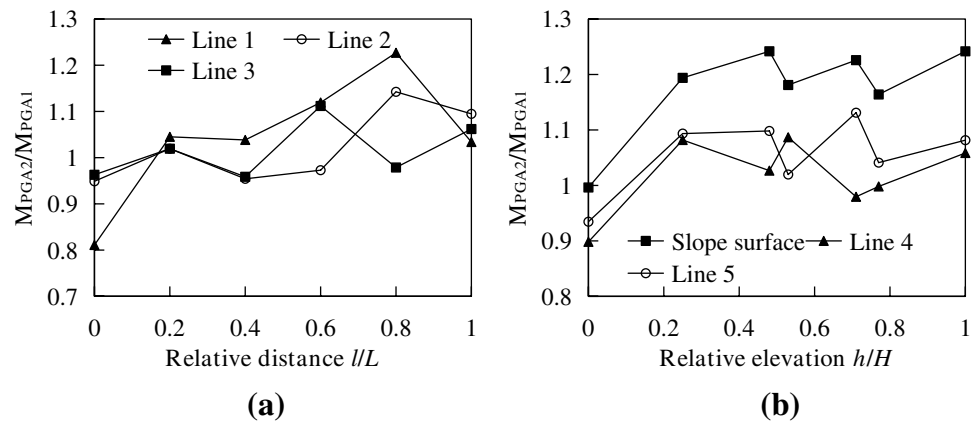
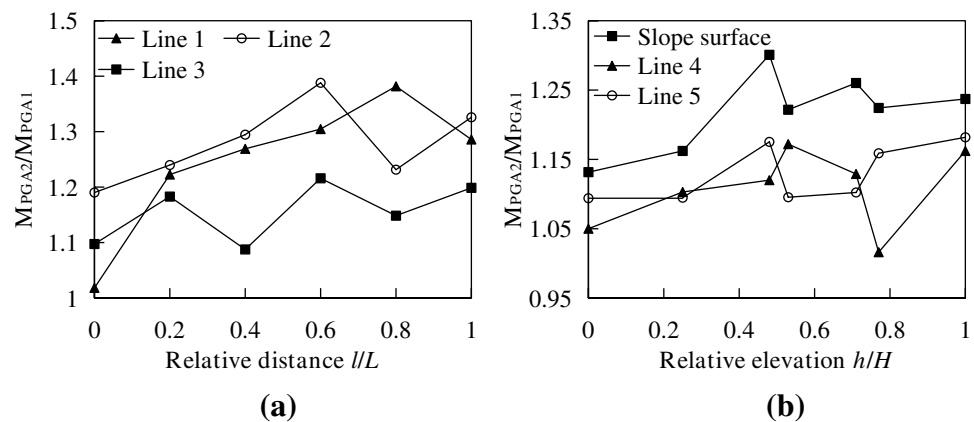


**Fig. 23**  $M_{PGA}$  ratio of Model 2 to Model 1 when input 0.1 g WE wave in- $z$  direction: **a** along the horizontal direction of the slope; **b** along the vertical direction of the slope



seismic wave propagation characteristics and propagation path of the bedrock are obviously changed due to the tunnel excavation, and then the dynamic response characteristics of the slope are changed accordingly.

In addition, to further investigate the influence of the tunnel structure on the dynamic response of the layered slope at the tunnel portal, the  $M_{PGA}$  ratio of Model 2 to Model 1 ( $M_{PGA2}/M_{PGA1}$ ) is shown in Figs. 22 and 23.  $M_{PGA2}/M_{PGA1}$  increases with elevation overall but shows a strong nonlinear increasing trend, which is closely related to the effect of the discontinuity of the rock mass and tunnel structure on the wave propagation characteristics. This is because there are a large number of discontinuous planes and empty surfaces in the tunnel slope. When the seismic wave propagates in the discontinuous planes and the tunnel, many refraction and reflection phenomena are generated, thus forming a complex seismic wave field, and its stress characteristics are more complex.  $M_{PGA2}/M_{PGA1}$  is greater than 1.0, overall, specifically, 1.0–1.25, which indicates that the tunnel structure makes the dynamic response of the layered slope have an obvious amplification effect.

Therefore, the interaction mechanism between the layered slope and the tunnel structure can be summarized as follows: Due to the interaction between the tunnel structure and seismic waves, the vertical wave and the horizontal wave reflected from the geological interface interfere with the tunnel, which changes the propagation direction of seismic waves, and the seismic waves propagate in the slope at different incident angles, resulting in local superposition and amplification effect of seismic waves in the rock mass. Due to the existence of a tunnel in the slope, a complex stress increment area will be formed inside the slope, resulting in the subsidence and deformation of the rock mass, thus affecting the overall stability of the slope.

## Conclusions

Two-dimensional FEM dynamic analysis is used to analyze the dynamic response characteristics of the two models subject to earthquake excitation. The following conclusions can be drawn:

1. Stratigraphic lithology and tunnel structure have impacts on wave propagation characteristics and propagation paths in slopes. In Model 1, waves in the bedrock show layered propagation characteristics and a significant amplification effect appears when waves propagate to the soft rock interface, and the waves gradually propagate to the infinite-element boundary at the slope crest. In Model 2, the tunnel structure caused a local amplification effect when waves propagated between the two tunnels. After entering the soft/hard rock strata, the waves propagated along the slope surface to the slope crest. Due to the difference between the tunnel and the surrounding rock, waves show obvious discontinuous propagation characteristics in the lining structure.
2. The slope surface, elevation, and ground motion directions affect the dynamic response of the slopes. The formation lithology has an influence on the dynamic amplification effect of the slope, and soft rock has the most obvious amplification effect. The closer the distance to the slope surface is along the horizontal direction, the greater the  $M_{PGA}$  is. In the vertical direction, the  $M_{PGA}$  increases with elevation overall. Compared with Model 1, the tunnel structure makes the  $M_{PGA}$  show obvious nonlinear variation characteristics and increases the  $M_{PGA}$  between the two tunnels. The amplification effect of the surface slope is greater than that of the internal slope. In Model 1, the  $M_{PGA}$  under the horizontal incident wave is greater than that of the vertical wave. In Model 2, the amplification effect under a vertical incident wave is much larger in the bedrock, while the amplification effect under a horizontal wave is greater in the soft and hard rock strata. For tunnels, the magnifying effect of vertical seismic waves is greater than that of horizontal waves.
3. The dynamic amplification effect of the tunnel lining structure is mainly concentrated in the adjacent areas of the two tunnels. The  $M_{PGA}$  of the right arch waist of the left tunnel and the left arch waist of the right tunnel is the largest, and the dynamic amplification effect of the left tunnel structure is greater than that of the right one. The tunnel structure has an influence on the dynamic response of the layered slope.  $M_{PGA2}/M_{PGA1}$  is 1.0–1.25, overall, indicating that the dynamic amplification effect of Model 2 is greater than that of Model 1. In Model 2, the tunnel structure increases the  $M_{PGA}$  of the slope. Because of the interaction of the tunnel structure, surrounding rock, and waves, the propagation path and law of seismic waves are changed, resulting in a change in the dynamic response characteristics of the slope.
4. However, the dynamic response of the tunnel-slope system is a scientific problem involving multiple domains. In this work, the acceleration dynamic response is used only in the time domain, and further exploration needs to be carried out in the frequency domain and time–fre-

quency domain. The discrete element method needs to be used to study the evolution law and seismic damage of the tunnel-slope system and to clarify its seismic failure mode.

**Acknowledgements** This study was funded by the National Natural Science Foundation of China (52109125 and 52208359), the China Postdoctoral Science Foundation (2020M680583), and the National Postdoctoral Program for Innovative Talent of China (BX20200191).

**Author contribution** Danqing Song performed the data analyses and wrote the manuscript; Zhuo Chen helped perform the analysis with constructive discussions; Zhizheng Guo, Mengxin Liu, Junfeng Tang, and Xiangang Jiang carried out subsequent numerical simulation.

**Funding** National Natural Science Foundation of China, 52109125, Danqing Song, 52208359, Zhuo Chen, China Postdoctoral Science Foundation, 2020M680583, Danqing Song, National Postdoctoral Program for Innovative Talent of China, BX20200191, Danqing Song

**Data availability** The raw/processed data required to reproduce these findings cannot be shared at this time as the data also forms part of an ongoing study.

## Declarations

**Conflict of interest** The authors declare no competing interests.

## References

- Bandini A, Berry P, Boldini D (2015) Tunnelling-induced landslides: the Val di Sambro tunnel case study. *Eng Geol* 196:71–87
- Chen Z, Song D (2020) Numerical investigation of the recent Chenhecun landslide (Gansu, China) using the discrete element method. *Nat Hazards* 105:717–733
- Ergün T (2018) Assessments on slope instabilities triggered by engineering excavations near a small settlement (Turkey). *J Mt Sci* 15(1):114–129
- Fan G, Zhang L, Zhang J, Yang C (2019) Analysis of seismic stability of an obsequent rock slope using time–frequency method. *Rock Mech Rock Eng* 52:3809–3823
- Fan JW, Zhang YF, Zhou WJ, Yin C (2022) Landslide-tunnel interaction mechanism and numerical simulation during tunnel construction: a case from expressway in Northwest Yunnan Province, China. *Arabian Journal of Geosciences* 15:1394
- Geli L, Bard PY, Jullien B (1988) The effect of topography on earthquake ground motion: a review and new results. *Bull Seismol Soc Am* 78(1):42–63
- Goodman RE, Taylor RL, Brekke T (1968) A model for the mechanics of jointed rock. *ASCE Soil Mechanics and Foundation Division Journal* 99(5):637–659
- Jiang X, Wang F, Sun YH, G, Niu J, (2018) Dynamic Response of Shallow-Buried Small Spacing Tunnel with Asymmetrical Pressure: Shaking Table Testing and Numerical Simulation. *Geotech Geol Eng* 36:2037–2055
- Kaya A, Karaman K, Bulut F (2017) Geotechnical investigations and remediation design for failure of tunnel portal section: a case study in northern turkey. *J Mt Sci* 14(06):1140–1160
- Konagai K, Numada M, Zafeirakos A, Johansson J, Sad A, Katagiri T (2005) An example of landslide-inflicted damage to tunnel in the 2004 Mid-niigata prefecture earthquake. *Landslides* 2(2):159–163

- Kuhlemeyer RL, Lysmer J (1973) Finite element method accuracy for wave propagation problems. *Journal of Soil Mechanics Foundations Div* 99(SM5):421–427
- Lei H, Wu HG, Qian JG (2023) Seismic failure mechanism and interaction of the cross tunnel-slope system using Hilbert-Huang transform. *Tunnelling and Underground Space Technology Incorporating Trenchless Technology Research* 131:104820
- Li Z, Huang H, Xue Y (2014) Cut-slope versus shallow tunnel: risk-based decision making framework for alternative selection. *Eng Geol* 176:11–23
- Li ZL, Li JC, Li W (2023) Evaluation of seismic response of tunnels near slope surfaces and performance of anti-seismic measures. *Soil Dyn Earthq Eng* 165:107734
- Liu H, Xu Q, Li Y, Fan X (2013) Response of high-strength rock slope to seismic waves in a shaking table test. *Bull Seismol Soc Am* 103(6):3012–3025
- Liu GW, Song DQ, Chen Z, Yang JW (2020) Dynamic response characteristics and failure mechanisms of coal slopes with weak intercalated layers under blasting loads. *Advances in Civil Engineering* 2020:5412795
- Madsen PA (1983) Wave reflection from a vertical permeable wave absorber. *Coast Eng* 7(4):381–396
- Ngo D, Scordelis AC (1967) Finite element analysis of reinforced concrete beams. *Journal Proceedings* 64(3):152–163
- Niu J, Jiang X, Wang F (2018) Stability analysis of rock slope with small spacing tunnel under earthquakes and influence of ground motion parameters. *Geotechnical Geological Engineering* 36:2437–2453
- Pai LF, Wu HG (2021) Multi-attribute seismic data spectrum analysis of tunnel orthogonal underpass landslide shaking table test. *Soil Dyn Earthq Eng* 150:106889
- Qi S, Qiang X, Lan H, Bing Z, Liu J (2011) Spatial distribution analysis of landslides triggered by 2008.5.12 wenchuan earthquake. *China. Engineering Geology* 116(1–2):95–108
- Qi W, Geng P, Chen CJ, Chen JB, He C (2023) Determination of seismic response of reinforced tunnel portal slope using shaking table tests. *Tunnelling and Underground Space Technology Incorporating Trenchless Technology Research* 136:105072
- Song D, Chen Z, Ke Y, Nie W (2020) Seismic response analysis of a bedding rock slope based on the time-frequency joint analysis method: a case study from the middle reach of the Jinsha River. *China Eng Geol* 274:105731
- Song D, Liu X, Chen Z, Chen J, Cai J (2021a) Influence of tunnel excavation on the stability of a bedded rock slope: a case study on the mountainous area in southern anhui, China. *KSCE J Civ Eng* 25:114–123
- Song D, Liu X, Huang J, Zhang J (2021b) Energy-based analysis of seismic failure mechanism of a rock slope with discontinuities using Hilbert-Huang transform and marginal spectrum in the time-frequency domain. *Landslides* 18:105–123
- Su J, Wang Y, Niu X, Sha S, Yu J (2022) Prediction of ground surface settlement by shield tunneling using XGBoost and Bayesian optimization. *Eng Appl Artif Intell* 114:105020
- Sun H, Wu HG, Ma ZG, Yuan Z, Feng K (2022) Analysis of Seismic Damage Modes of Landslides Containing Tunnels under Horizontal Earthquake Action. *Geofluids* 2022:6026316
- Wang G, Huang R, Louren OS, Kamai T (2014) A large landslide triggered by the 2008 wenchuan (m8.0) earthquake in donghekou area: phenomena and mechanisms. *Eng Geol* 182:148–157
- Wang F, Jiang X, Niu J, Yang H (2018) Experimental study on seismic dynamic characteristics of shallow-bias tunnel with a small space. *Shock Vib* 2018:6412841
- Wang DY, Yuan JX, Cui GY, Liu J, Wang HF (2020a) Experimental study on characteristics of seismic damage and damping technology of absorbing joint of tunnel crossing interface of soft and hard rock. *Shock Vib* 2020:1–13
- Wang ZF, Shi FG, Li DD, Li H (2020b) Tunneling-induced deep-seated landslides: a case study in gulin county, sichuan, china. *Arab J Geosci* 13(19):1039
- Wang Q, Geng P, Chen C, Chen J, He C (2023) Determination of seismic response of reinforced tunnel portal slope using shaking table tests. *Tunn Undergr Space Technol* 136:105072
- Zhang C, Han K, Zhang D (2015) Face stability analysis of shallow circular tunnels in cohesive–frictional soils. *Tunn Undergr Space Technol* 50:345–357
- Zhang Z, Zhao Q, Xu C, Xu X (2017) Interaction analyses between tunnel and landslide in mountain area. *J Mt Sci* 14:1124–1139
- Zhang ZG, Fang L, Zhao QH, Zhang MX, Pan YT, Ma BB (2022) An experimental evaluation of pile-anchor strengthening mechanics for existing tunnels in landslide region. *Underground Space* 7(2):199–218
- Springer Nature or its licensor (e.g. a society or other partner) holds exclusive rights to this article under a publishing agreement with the author(s) or other rightsholder(s); author self-archiving of the accepted manuscript version of this article is solely governed by the terms of such publishing agreement and applicable law.